Lasers in Manufacturing Conference 2023

Process monitoring during ultrafast laser processing by means of soft X-ray emission

Julian Holland[a,*], Rudolf Weber[a], Christian Hagenlocher[a], Thomas Graf[a]

ᵃ Institut für Strahlwerkzeuge, Universität Stuttgart, Pfaffenwaldring 43, 70569 Stuttgart, Germany

Abstract

Soft X-ray emission is a well-established phenomenon that occurs during laser material processing with ultrafast lasers at high irradiances. The emitted radiation spectrum provides details about the irradiance at the interaction zone of the laser beam and the processed material, making it a valuable beam diagnostic tool. However, quick measurements of the X-ray emission are necessary to make use of the spectral information. Unfortunately, these measurements are frequently hindered by energy pile-up because of the short emission times and high photon fluxes that occur during each laser pulse. A spectrometer was employed to measure the spectral X-ray emission produced by laser processing at irradiances of up to $1.6 \cdot 10^{14}$ W/cm² and a de-piling algorithm was used to derive the underlying pile-up free spectrum. These spectra were obtained at various focal positions to determine the corresponding local irradiance and thereby analyze the focusing properties of the laser beam. Utilizing the spectral X-ray emission allows for the measurement of beam properties at the highest average power and pulse energy attainable with modern laser systems.

Keywords: X-ray; ultrafast laser; diagnostics; spectroscopy; process-control

1. Introduction

Characterizing laser beam properties and thus the laser process itself at maximum pulse energy and average power presents a significant challenge. Modern laser systems provide hundreds of Watts of average power, which results in irradiances exceeding 10^{13} W/cm² on the sample surface, as demonstrated by Negel et al., 2016 and Nubbemeyer et al., 2017. Under these conditions, beam propagation through the atmospheric environment is significantly impaired by factors like air breakdown, as described by Sprangle et al., 2002 or thermal lensing, as investigated by Faas et al., 2018. Both, air breakdown and thermal lensing results in changes of the focusing and, consequently, local irradiance.

It is known that such high irradiances lead to the formation of a hot plasma during materials processing which was shown by Gamaly and Rode, 2013 and Giulietti and Gizzi, 1998. A portion of the plasma electrons is heated to extremely high temperatures, reaching average kinetic energies of several keV. These highly energetic electrons, known as "hot electrons," interact with ions, producing Bremsstrahlung emission,

recombination radiation, and line emission in the soft X-ray energy range, as proven by Giulietti and Gizzi, 1998. However, the X-ray emission can serve as a diagnostic tool for laser beam analysis, as its spectrum contains valuable information about the actual irradiance on the surface of the sample. To effectively utilize this emission as a beam diagnostic tool, rapid spectral measurements are necessary.

However, performing fast spectral measurements of the soft X-ray emission during ultrafast laser processing poses challenges due to the short emission times within the pulse duration range. One significant challenge is the phenomenon called "pile-up," which occurs when multiple photons hit the detector simultaneously during processing, resulting in a single event being registered with higher energy. This issue has been addressed by the algorithm of Holland et al., 2023, which enables rapid spectral measurements using a PIN-detector. The algorithm calculates the underlying Pile-Up free spectrum for any measured X-ray spectrum during ultrafast laser processing.

As proven by Weber et al., 2019the Pile-Up free X-ray spectrum provides information about the actual irradiance at the interaction zone between the laser beam and the processed material. While certain laser parameters such as average power, pulse frequency, and raw beam diameter are well-known, X-ray measurements offer insights into determining pulse duration, focal diameter, M² (beam quality factor), and the true focal width of the focusing optic. Thus, understanding the X-ray spectrum during laser processing allows for precise monitoring and control of laser parameters with maximum sensitivity.

In this publication, a method is presented to determine the beam diameter on the processed surface by means of X-ray measurements at high pulse energy. The results are compared to the expected values by using the formulas as well as measurements of single line ablation, which were analyzed with a microscope afterward.

2. Experimental setup

The experiments utilized a Ti:Sapphire laser (Spitfire ACE, Spectra Physics) that generated pulses ranging from 75 fs to 6 ps, with a maximum pulse energy of up to 7 mJ at a wavelength of 800 nm (FWHM = 30 nm). The laser operated at a constant repetition rate of 1 kHz. To focus the laser beam, an F-Theta lens with a focal length of 400 mm was used, resulting in a diameter d_0 of at least 46 µm at the focal position.
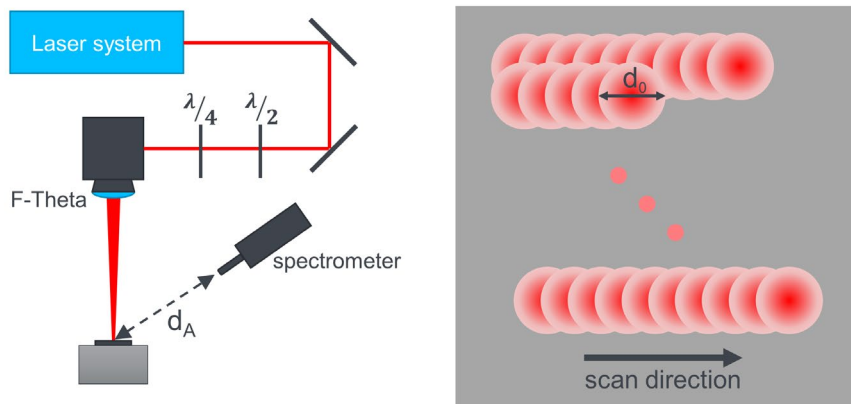

Fig. 1. Experimental setup. The laser beam was focused by means of an F-Theta lens in combination with a laser scanner to perform line scanning ablation. The scan direction was kept constant during the measurements and only one layer was processed.

The focal position in relation to the sample surface was varied from -1 mm to +5 mm at three different average powers (1 W, 1.5 W and 3 W). The pulse duration was set to 1 ps for all experiments

During the experiment, the laser was directed over the surface of a stainless-steel (1.4301) sample. The pulse overlap was set at 80%, while the scanning line overlap was set at 75%, as this configuration was reported by Legall et al., 2019 to generate the highest X-ray emission. Additionally, this laser processing technique prevented the formation of deep grooves, which could attenuate the X-ray emission. By avoiding deep grooves, the X-ray radiation was able to reach the detector without significant obstruction from the surrounding material. For each measurement, an additional line was processed and measured afterward by means of an optical microscope (VK 9700, Keyence Corporation, Osaka, Japan).

The X-ray emission was measured by means of a spectrometer (XRS Detector System, PN Detector) at a fixed distance d_A of 30 cm for all experiments. The spectrometer was a silicon drift detector (SDD), had an active area of 30 mm², a thickness of 450 μm and was covered with an 8 μm thick beryllium foil to keep the system light tight. The beam path and the detector's position are shown on the left and the processing strategy on the right of Fig. 1.

3. Results

The evaluation of the experimental data consists of determining the focal diameter of the laser on the material surface in three different ways.

3.1. Focal diameter calculated by given laser parameters

First. the diameter d was calculated from the given laser parameters and the focusing optics by

$$d_0 = \frac{4M^2\lambda f}{\pi d_L} \tag{1}$$

where M² is the beam quality factor, λ the wavelength of the laser, f is the focal length of the focusing F-Theta lens, and d_L is the diameter of the beam on the lens. The calculated results for the focal diameter are shown in Fig. 2 as black squares with the error bars referring to ±10% of the expected calculated value.

3.2. Focal diameter determined from ablated line scan

To determine the diameter from the ablation a single line was scanned with the laser parameters, which were used to perform the experiments. The diameter d_{abl} of the line ablation was measured, by means of a light microscope. The diameter d_0 of the focal spot then was determined by using

$$d_{abl} = d_0 \cdot \sqrt{\frac{1}{2} ln\left(\frac{2\eta_{abs}E_P}{\pi \ell_0 h_V \, d_0^2/4}\right)}, \tag{2}$$

where η_{abs} is the absorption coefficient, E_P the laser pulse energy, ℓ_0 the optical penetration depth and h_V the volume-specific enthalpy for evaporation of the processed material, as stated by Holder et al., 2022. Focal diameter determined from spectral X-ray emission

The X-ray emission is mainly determined by the temperature of the hot electrons in the plasma which depends on the irradiance and the used laser wavelength. The scaling law used in this publication is

$$T_h = 4.1 \cdot 10^{-5} (\lambda^2 I_0)^{0.53} \tag{3}$$

which is given by Weber et al., 2019 as a good fit for irradiances in the region of 10^{13} W/cm² up to several 10^{14} W/cm². With this temperature, the emission spectrum can be described by

$$E(\omega) = T_A(\omega, d_A) T_F(\omega, d_F) c_E(V_P, n_h, Z_i) \sqrt{\frac{1}{k_B T_h}} e^{-\frac{\hbar\omega}{k_B T_h}} \tag{4}$$

where $\hbar$ and k_B are the Planck constant divided by 2π and the Boltzmann constant, respectively. Further c_E is a pre-factor, which depends on volume V_P, the degree of ionization Z_i as well as the hot electron number density n_h of the plasma as it was shown by Giulietti and Gizzi, 1998 and Weber et al., 2019. T_A and T_F are the energy-dependent transmission coefficients through a distance d_A of air and any filter material of a given thickness d_F, respectively which were calculated using the atomic form factor data from Seltzer, 1995.

By using the de-piling algorithm, presented by Holland et al., 2023, the measured spectral data, which may suffer from energy pile-up, were used to determine the true, pile-up free X-ray emission spectrum. With this spectrum, the irradiance on the surface in the processing region was calculated following eq. (3) and (4). The corresponding beam diameter d_0 was calculated by

$$d_0 = \frac{8 E_P}{\tau_P I_0} \sqrt{\frac{\ln(2)}{\pi^3}} \tag{5}$$

where τ_P is the pulse duration.

The data points in Fig. 2 compare the three differently determined beam diameters as function of the position of their beam waist. The local Beam diameter is shown as a function of the position of the beam waist. The calculated results for the expected focal diameter are shown in Fig. 2 as black squares with the error bars referring to ±10% of the expected calculated value. The results of the measurements of the ablated diameter are represented by the red circles in Fig. 2. The error bars are determined to be ±30%, which results from variations in the absorption coefficient as well as errors by determining the edge of the ablated line on the material. The beam diameters determined by the X-ray emission are represented by the blue triangles and their error bars are estimated to be ±35% due to the uncertainties in determining the temperature of the hot electrons from the spectral data and the scaling of this temperature with the irradiance.
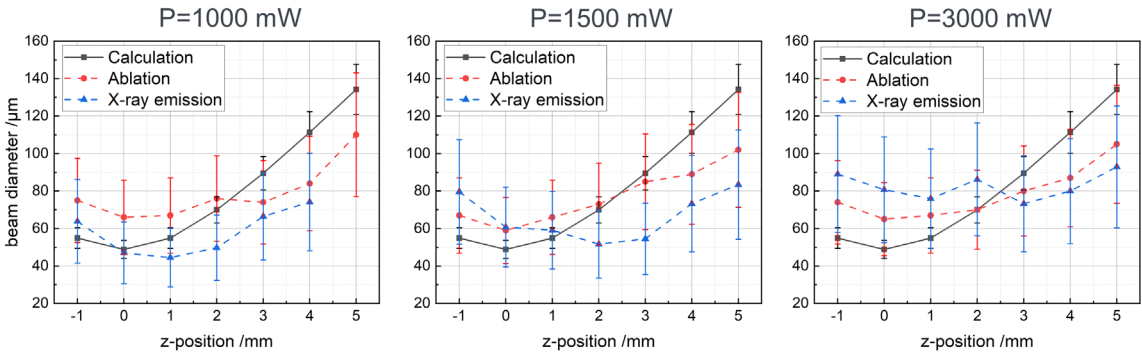

Fig. 2. Expected beam diameter (black squares), measured ablation diameter (red circles), and beam diameter determined from X-ray spectra (blue triangles) in case of processing a stainless-steel surface with an average power of 1000mW (left), 1500 mW (middle), and 3000 mW (right).

The results show that the beam diameter determined from the X-ray emission agrees well with the ablation diameter. However, both diameters, determined from the ablation as well as from the X-ray emission spectrum, differ from the expected calculated value. At the highest average power used (Fig. 2, right), both measurements show a shift of the smallest diameter to focal positions above the material surface, which can be caused by the self-focusing effect of the laser plasma For 1000 mW and 1500 mW of average power (Fig. 2, left and middle) the focal diameter, calculated from the X-ray emission is smaller than the resulting one from the measurements of the ablation. A characteristic beam caustic is visible for all used average powers. The focal region as well as the smallest focal diameter are broadening with increasing average power. These effects can be caused by self-focusing due to the plasma or air breakthrough due to the high irradiation in the region of the focal plane of the laser beam. Despite the slight quantitative uncertainty of the measurements, this information provide a valuable monitoring signal to monitor the focal position during the ablation process and to ensure highest process quality.

4. Conclusion

It was shown that the spectral X-ray emission from laser processing can be used to characterize the laser beam and thus the laser process itself at the highest average power and maximum pulse energy. The results show a clear laser caustic which is in good agreement with measurements of the corresponding ablation. The main benefits of measuring beam parameters by means of spectral X-ray emission are the sensitivity on the laser processing parameters as well as the small time, which is needed to perform such a measurement, which is in the region of some seconds by using modern laser systems with hundreds of kHz of pulse repetition rate. The X-ray emission and the presented analysis are potentially a valuable tool to monitor laser material processing for the sake of quality assurance.

Acknowledgments

References

Del Pizzo, V.; Luther-Davies, B.; Siegrist, M. R., 1977. On the generation of high flux densities within absorbing plasmas due to self-focussing of a laser beam, Appl. Phys. 14 4, p. 381

Faas, Sebastian; Foerster, Daniel J.; Weber, Rudolf; Graf, Thomas, 2018. Determination of the thermally induced focal shift of processing optics for ultrafast lasers with average powers of up to 525 W, Opt. Express 26 20, p. 26020

Gamaly, E. G.; Rode, A. V., 2013. Physics of ultra-short laser interaction with matter: From phonon excitation to ultimate transformations, Progress in Quantum Electronics 37 5, p. 215

Giulietti, Danilo; Gizzi, Leonida A., 1998. X-ray emission from laser-produced plasmas, Riv. Nuovo Cim. 21 10, p. 1

Holder, Daniel; Weber, Rudolf; Graf, Thomas, 2022. Analytical Model for the Depth Progress during Laser Micromachining of V-Shaped Grooves, Micromachines 13 6

Holland, Julian; Weber Rudolf; Graf Thomas, 2023. Fast spectral measurement of soft x-ray emission from ultrafast laser processing. In:. High-Power Laser Materials Processing: Applications, Diagnostics, and Systems XII: SPIE (12414), p. 13

Legall, Herbert; Schwanke, Christoph; Bonse, Jörn; Krüger, Jörg, 2019. The influence of processing parameters on X-ray emission during ultra-short pulse laser machining, Appl. Phys. A 125 8, p. 1

Negel, Jan-Philipp; Loescher, André; Bauer, Dominik; Sutter, Dirk; Killi, Alexander; Ahmed, Marwan Abdou; Graf, Thomas, 2016. Second Generation Thin-Disk Multipass Amplifier Delivering Picosecond Pulses with 2 kW of Average Output Power, Advanced Solid State Lasers, ATu4A.5

Nubbemeyer, Thomas; Kaumanns, Martin; Ueffing, Moritz; Gorjan, Martin; Alismail, Ayman; Fattahi, Hanieh et al., 2017. 1 kW, 200 mJ picosecond thin-disk laser system, Opt. Lett., OL 42 7, p. 1381

Seltzer, Stephen, 1995. Tables of X-Ray Mass Attenuation Coefficients and Mass Energy-Absorption Coefficients, NIST Standard Reference Database 126

Sprangle, Phillip; Penano, J. R.; Hafizi, Bahman, 2002. Propagation of Intense, Short Laser Pulses in the Atmosphere, Defense Technical Information Center, Fort Belvoir, VA

Weber, Rudolf; Giedl-Wagner, Roswitha; Förster, Daniel J.; Pauli, Anton; Graf, Thomas; Balmer, Jürg E., 2019. Expected X-ray dose rates resulting from industrial ultrafast laser applications, Appl. Phys. A 125 9, p. 1